



1 Potential environmental impact of bromoform from
2 Asparagopsis farming in Australia

3
4 Yue Jia^{1, a}, Birgit Quack^{2*}, Robert D. Kinley³, Ignacio Pisso⁴, Susann Tegtmeier¹

5
6 ¹ Institute of Space and Atmospheric Studies, University of Saskatchewan, Saskatoon, Canada

7 ² GEOMAR Helmholtz Centre for Ocean Research Kiel, Kiel, Germany

8 ³ Commonwealth Scientific and Industrial Research Organisation (CSIRO), Agriculture and Food,
9 Townsville, QLD 4811, Australia

10 ⁴ Norwegian Institute for Air Research (NILU), Kjeller, Norway

11 ^a *now at*: Cooperative Institute for Research in Environmental Sciences (CIRES), University of
12 Colorado Boulder, Boulder, CO, USA.

13 **Corresponding to*: B. Quack (bquack@geomar.de)

14

15

16

17

18

19



20 **Abstract**

21

22 To mitigate the rumen enteric methane (CH_4) produced by ruminant livestock, *Asparagopsis*
23 *taxiformis* is proposed as an additive to ruminant feed. During the cultivation of *Asparagopsis*
24 *taxiformis* in the sea or in terrestrial based systems, this macroalgae, like most seaweeds and
25 phytoplankton, produces a large amount of bromoform (CHBr_3), which may contribute to ozone
26 depletion once released into the atmosphere. In this study, the impact of CHBr_3 on the stratospheric
27 ozone layer resulting from potential emissions from proposed *Asparagopsis* cultivation in
28 Australia is assessed by weighting the emissions of CHBr_3 with the ozone depletion potential
29 (ODP), which is traditionally defined for long-lived halogens but has been also applied to very
30 short lived substances (VSLs). An annual yield of $\sim 3.5 \times 10^4$ Mg dry weight (DW) is required
31 to meet the needs of 50% of the beef feedlot and dairy cattle in Australia. Our study shows that the
32 intensity and impact of CHBr_3 emissions varies dependent on location and cultivation scenarios.
33 Of the proposed locations, tropical farms near the Darwin region are associated
34 with largest CHBr_3 ODP values. However, farming of *Asparagopsis* using either ocean or
35 terrestrial cultivation systems at any of the proposed locations does not have potential to impact
36 the ozone layer. Even if all *Asparagopsis* farming was performed in Darwin, the emitted CHBr_3
37 would amount to less than 0.016% of the global ODP-weighted emissions. The remains are
38 relatively small even if the intended annual yield in Darwin is scaled by a factor 30 to meet
39 the global requirements, which will increase the global ODP-weighted emissions by 0.48%

40

41



42 1. Introduction

43

44 Livestock is responsible for about 15% total anthropogenic greenhouse gas (GHG) emissions
45 (Gerber et al., 2013), ranking it amongst the main contributors to climate change. The global
46 demand for red meat and dairy is expected to increase >50% by 2050 compared to 2010 level, thus
47 mitigation measures to reduce the GHG emission from the global livestock industry are in high
48 demand (Beauchemin et al., 2020). Total GHG emissions from ruminant livestock contribute
49 about 18% of the total global carbon dioxide equivalent (CO₂-eq) inventory as CH₄ (Herrero and
50 Thornton, 2013). With a global warming potential 28 times higher than carbon dioxide (CO₂) and
51 a much shorter lifetime (~10 years, IPCC, 2014), ruminant enteric CH₄ is an attractive and feasible
52 target for global warming mitigation.

53 Enteric CH₄ from ruminant livestock is produced and released into the atmosphere through rumen
54 microbial methanogenesis (Morgavi et al., 2010). Methanogenic archaea (methanogens) intercept
55 substrate CO₂ and H₂ liberated during bacterial fermentation of feed materials (Kamra, 2005), and
56 during this inefficiency of the digestion process (Herrero and Thornton, 2013; Patra, 2012),
57 methanogen metabolism leads to reductive CH₄ production and loss of feed energy as CH₄
58 emissions. To abate enteric methanogenesis, different strategies such as feeding management and
59 antimethanogenic feed ingredients, have been proposed and assessed (e.g., Moate et al., 2016;
60 Mayberry et al., 2019; Beauchemin et al., 2020). Some types of macroalgae have been
61 demonstrated to mitigate production of CH₄ during *in vitro* and *in vivo* rumen fermentation
62 significantly (Kinley and Fredeen 2015; Li et al., 2018; Kinley et al., 2020; Abbott et al., 2020).
63 Among the different macroalgae species, Kinley et al. (2016a) concluded that the red algae
64 *Asparagopsis* spp. showed the most potential for CH₄ production decrease. Kinley et al. (2016b)
65 further demonstrated that forage with the addition of 2% *Asparagopsis taxiformis* could eliminate
66 CH₄ production *in vitro* without negative effects on forage digestibility. In recent animal
67 experiments, reduction of enteric CH₄ production by more than 98% was achieved with only 0.2%
68 addition of freeze-dried and milled *Asparagopsis taxiformis* to the to the organic matter (OM)
69 content of feedlot cattle feed (Kinley et al., 2020).

70 Halogenated, biologically active secondary metabolites are pivotal in the reduction of CH₄ induced
71 by *Asparagopsis* (Abbott et al., 2020). Most of the reduction is ascribed to bromoform (CHBr₃)
72 inhibition of the CH₄ biosynthetic pathway within methanogens (Machado et al., 2016). CHBr₃ as



73 a natural halogenated volatile organic compound originates from chemical and biological sources
74 including marine phytoplankton and macroalgae (Carpenter et al., 2000; Quack and Wallace,
75 2003). When emitted to the atmosphere, CHBr_3 has an atmospheric lifetime shorter than six months
76 and is often referred to as a very short-lived substance (VSLs). The halogenated VSLs have
77 drawn considerable interest because of their potential to deplete stratospheric ozone (Engel and
78 Rigby, 2018). Bromoform is the dominant compound among bromine-containing VSLs
79 emissions, resulting mostly from natural sources (Quack and Wallace, 2003) and to a lesser degree
80 from anthropogenic production (Maas et al., 2019; 2021). With an atmospheric lifetime of about
81 17 days (Carpenter and Reimann, 2014), CHBr_3 can deliver bromine to the stratosphere under
82 appropriate conditions of emission strength and vertical transport (e.g., Aschmann et al., 2009;
83 Liang et al., 2010; Tegtmeier et al., 2015, 2020) and thus contribute to ozone depletion at middle
84 and high altitudes (e.g., Yang et al., 2014; Sinnhuber and Meul, 2015). Global research on enabling
85 large-scale seaweed *Asparagopsis* farming is increasing (Black et al., 2021) as it appears to be one
86 of the most promising options as an antimethanogenic feed ingredient to achieve carbon neutrality
87 in the livestock sector within the next decade (Kinley et al., 2020; Roque et al., 2021). In
88 consequence, the environmental impact of CHBr_3 due to *Asparagopsis* farming also needs to be
89 explored and elucidated.

90 The hypothesis was that large scale cultivation of *Asparagopsis* would not contribute significantly
91 to depletion of the ozone layer. The aim of this study was elucidation of anthropogenic and natural
92 processes that may contribute to CHBr_3 emissions inherent in large scale production of
93 *Asparagopsis spp.* and the subsequent impact of CHBr_3 release to the atmosphere by using
94 cultivation in Australia as the model. Specific objectives were to inform the industry on: (i) the
95 potential impact of CHBr_3 associated with mass production of *Asparagopsis* on atmospheric
96 halogen budgets and ozone depletion; (ii) potential impacts relative to variability in regional
97 climate, atmospheric conditions, and convection trends with different potentials for transport of
98 CHBr_3 to stratospheric ozone; (iii) the combined CHBr_3 emissions potential of ocean and terrestrial
99 based cultivation of *Asparagopsis* to supply sufficient biomass for up to 50% of beef feedlot and
100 dairy cattle in Australia; and (iv) extrapolation of the impacts of production to requirements on a
101 global scale.

102

103 2. Data and Method

104



105 The potential impact of CHBr_3 on the atmospheric bromine budget and stratospheric ozone
106 depletion, associated with *Asparagopsis spp.* mass production was assessed for assumed annual
107 yields and particular production scenarios of macroalgae in Australia. Terrestrial systems
108 cultivation and open ocean cultivation under different harvest conditions, variations of seaweed
109 yield and growth rates for various scenarios and locations were tested as described in the following
110 subsections.

111 2.1 Cultivation Scenarios

112
113 The cultivation scenarios in this study assume that sufficient seaweed is grown to supply
114 *Asparagopsis spp.* to 50% of the Australian herds of beef cattle in feedlots (100%: $\sim 1.0 \times 10^6$) and
115 dairy cows (100%: $\sim 1.5 \times 10^6$). For a effective reduction of CH_4 production from ruminants, a 0.38%
116 addition of freeze-dried and milled *Asparagopsis taxiformis* to the daily feed dry matter intake
117 (DMI) is required (Kinley et al., 2020). This results in daily feed additions of 38 g dry weight (DW)
118 *Asparagopsis* per head of feedlot cattle and 94 g DW *Asparagopsis* per head of dairy cows. In
119 total, the required annual yield amounts to 3.4674×10^4 Mg DW *Asparagopsis* to supplement the
120 feed of roughly 50% of the Australian feedlot cattle and Australian dairy cows. Assuming that
121 fresh weight (FW) has a DW content of 15%, a total of 2.3116×10^5 Mg FW *Asparagopsis* needs
122 to be harvested every year.

123 For a global scenario, we make the functional assumptions that: (i) there would be adoption of 30%
124 of the global feed base to be supplemented with *Asparagopsis* farmed in Australia to reduce
125 ruminant CH_4 production worldwide; (ii) *Asparagopsis* would be adopted by 50% of Australia's
126 feedlot and dairy industries; and (iii) this is approximately equivalent to 1% of the global feedlot
127 and dairy herds for the purpose of both assumed magnitude of production and adoption relevant
128 for calculations of supply and emissions. This export scenario requires for 30 times increased
129 production compared to the Australian scenario if all the required *Asparagopsis* was to be cultivated
130 in Australia and an annual harvest of ~ 1 Tg DW *Asparagopsis* would be needed from Australian
131 waters.

132 For the future farm distributions in Australia, we assume that *Asparagopsis* will be cultivated in
133 open ocean systems and terrestrial confinement systems (that may include, but not limited to, tanks,
134 raceways, and ponds) located near Geraldton, Triabunna, and Yamba (Figure 1). We assume that



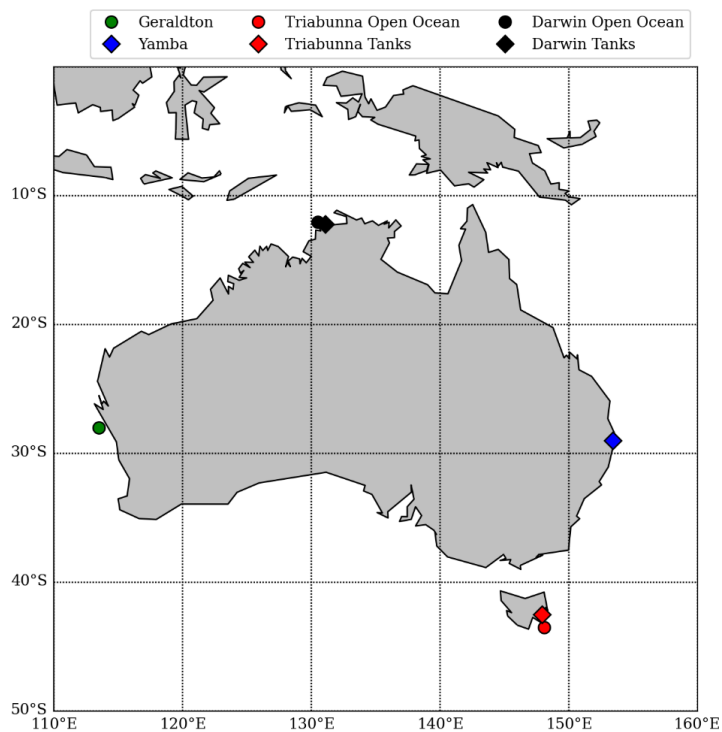
135 one third of the required annual yield ($=1.1558 \times 10^4$ Mg DW) is grown near Triabunna (T), with
136 60% in terrestrial systems and 40% in open ocean farms, one third is grown in terrestrial systems
137 at Yamba (Y), and the last third is grown in the open ocean in Geraldton (G). For comparison of
138 the environmental impact, we also adopt a tropical scenario where all farms with their total annual
139 yield of 3.4674×10^4 Mg DW are assumed to be situated near Darwin.

140 The emissions of CHBr_3 from the macroalgae farms can be derived based on estimates of the
141 standing stock biomass. For any given farming scenario, the standing stock biomass B_f (g DW) is
142 a function of time t and can be calculated from the initial biomass B_i (g DW) and the specific
143 growth rate GR (%/day) according to Hung et al. (2009):

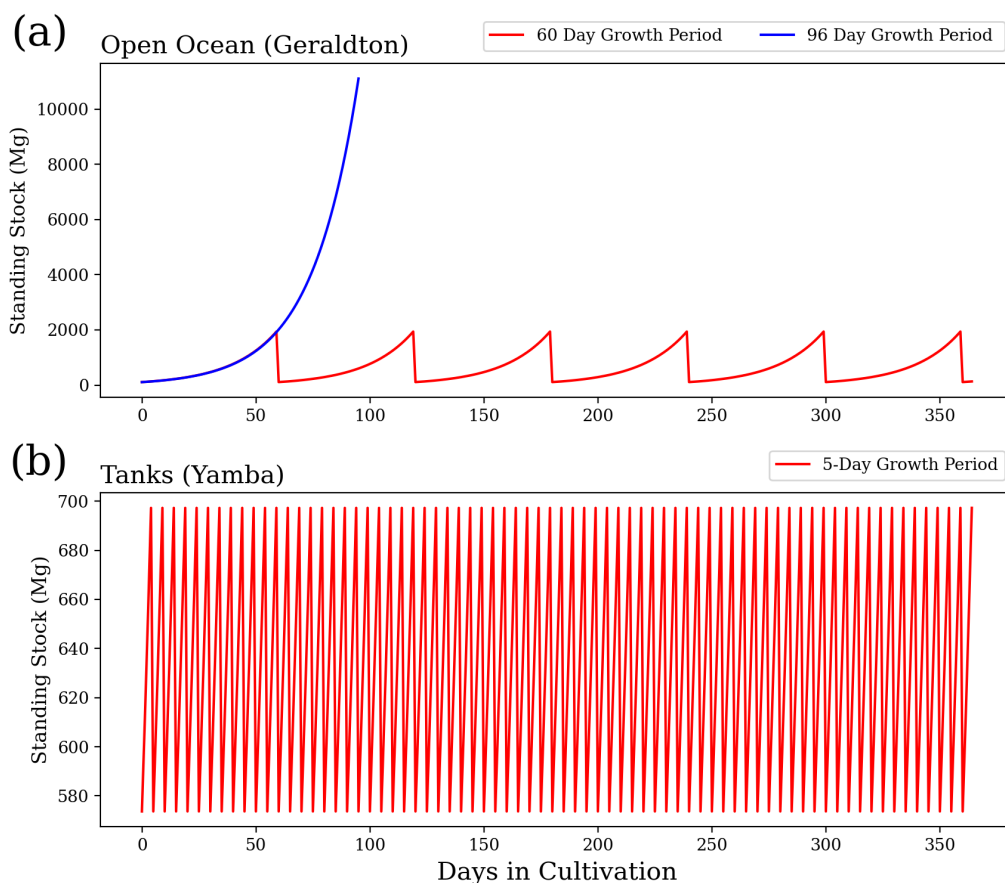
$$144 \quad B_f(t) = B_i \cdot (1 + GR/100)^t \quad (1)$$

145 Terrestrial systems and open ocean cultivation scenarios are assuming a fixed targeted annual yield.
146 For a given initial biomass and growth rate, the length and frequency of the growth periods per
147 year need to be chosen accordingly, to achieve the required final yield. Yong et al., (2013) checked
148 the reliability of different equations for seaweed growth rate determination by comparing the daily
149 seaweed weight cultivated under optimized growth condition, and the most reliable relationship
150 between initial and final weight leads to the form of Eq (1). We also applied several growth rates
151 from 1 to 10% to show the possible influence of this parameter on the overall emissions of the
152 algae. Average growth rates of *Asparagopsis* ranged from 7 to 13 %/day in samples from tropical
153 and sub-tropical Australia during short-term experiments (Mata et al., 2017). We used a lower
154 growth rate of 5% for our scenario to provide an upper estimate of potential CHBr_3 emissions.
155 Note that emissions decrease by 27% when using a growth rate of 7% as demonstrated in section
156 3.1.

157 Figure 2 provides an example of the variations of standing stock of *Asparagopsis* for the farms of
158 Geraldton (all open ocean) and Yamba (all terrestrial systems) with a growth rate of 5% per day.
159 For the open ocean cultures, we assume a scenario of six harvests per year and 60 day growth
160 periods to obtain the annual yield (Elsom, 2020). For a sensitivity study, we assume an alternative
161 scenario based on the same initial biomass, but only one harvest per year. As evident from Figure
162 2, the same annual yield can be achieved with one harvest per year if applying an extended growth
163 period of 96 days. For the tank cultures, a harvest every 5 days (73 harvests per year) is assumed
164 as a realistic scenario (Elsom, 2020).



165
166 **Figure 1.** Locations of actual and theoretical *Asparagopsis* farms in Geraldton, Triabunna, Yamba,
167 and Darwin.



168
169 **Figure 2.** Standing stock biomass of *Asparagopsis* cultivation a) in the open ocean for a 60-day
170 growth period and 96 day growth period and b) in terrestrial systems culture for a 5 day growth
171 period. Each of the three scenarios will achieve an annual yield of 1.1558×10^4 Mg DW.

172
173 **2.2 *Asparagopsis* CHBr₃ release rates**

174
175 Rates of the CHBr₃ content in *Asparagopsis* given in the literature range between 3.4 to 43 mg
176 CHBr₃/g DW, with values around 10 mg CHBr₃/g DW appearing to be realistic in current
177 cultivation (Burreson and Moore, 1976; Mata et al., 2012, 2017; Paul et al., 2006; Vucko et al.,
178 2017). We assume that *Asparagopsis* strain selection cultivated for feed supplements will lead to
179 high yielding CHBr₃ varieties thus we assume augmented CHBr₃ production with a mean content



180 of 21.7 mg $\text{CHBr}_3/\text{g DW}$ (Magnusson et al., 2019) for this study.
181 Very few values on the CHBr_3 release from *Asparagopsis* have been reported in the literature. A
182 constant release of 1100 ng $\text{CHBr}_3/\text{g DW hr}^{-1}$ was measured for *Asparagopsis armata*
183 *tetrasporophyte*, which has a CHBr_3 content of 14.5 mg $\text{CHBr}_3/\text{g DW}$ (Paul et al., 2006). We
184 assume a linear scaling between the CHBr_3 release rates and the content. Thus, a cultivated
185 *Asparagopsis* for which we assume 21.7 mg $\text{CHBr}_3/\text{g DW}$ should release around 1646 ng CHBr_3/g
186 DW hr^{-1} , a rate which has been confirmed by Marshall et al. (1999). Therefore, for our calculations,
187 we assume a constant release of 1600 ng $\text{CHBr}_3/\text{g DW hr}^{-1}$ for farmed *Asparagopsis* with a CHBr_3
188 content of 21.7 mg $\text{CHBr}_3/\text{g DW}$. These content and release rates are higher than for wild stock
189 algae (Leedham et al., 2013; Nightingale et al., 1995) as the farming aims at high yielding CHBr_3
190 varieties. As available information on this topic is very sparse no variations of the release rate with
191 life-cycle stages, season, location, or other environmental parameters was used in this study. Also,
192 the two species *Asparagopsis armata* and *Asparagopsis taxiformis* were treated the same way as
193 *Asparagopsis spp.*, as variations in CHBr_3 content and release within or between species are
194 currently unknown (Mata et al., 2017) and more research on this topic is needed.

195

196 2.3 Parameterization of CHBr_3 Emission

197

198 The emissions of CHBr_3 from farmed macroalgae are a function of the standing stock biomass (in
199 g DW) and can be calculated with the constant release rate (R_{CHBr_3}) of 1600 ng $\text{CHBr}_3/\text{g DW hr}^{-1}$
200 multiplied with the standing stock. The total release of CHBr_3 (E_{CHBr_3}) over the complete growth
201 period of T days is given by the integral over the daily emissions from day 1 to day T:

$$202 \quad E_{\text{CHBr}_3} = \int_0^T 24 \cdot B_i \cdot (1 + GR)^t \cdot R_{\text{CHBr}_3} dt = 24 \cdot B_i \cdot R_{\text{CHBr}_3} \cdot \frac{[(1+GR)^T - 1]}{\ln(1+GR)} \quad (2)$$

203 For our atmospheric impact studies we assume, that all CHBr_3 released from the algae is emitted
204 into the atmosphere at its location of production. An increasing seawater concentration of CHBr_3
205 shifts the equilibrium conditions between seawater and air towards the atmosphere, as CHBr_3
206 easily volatilizes to the atmosphere. Consequently, air-sea exchange acts as a relatively fast loss
207 process for CHBr_3 in surface water. Oceanic sinks can also impact CHBr_3 , but act on relatively
208 long timescales. Degradation through halide substitution and hydrolysis results in the ocean sink
209 CHBr_3 half-life of 4.37 years (Hense and Quack, 2009). Thus, most of the CHBr_3 contained in



210 surface seawater is instantly outgassed into the atmosphere without oceanic loss processes playing
211 a role as confirmed by the modelling study of Maas et al. (2020).

212 The air-sea exchange of CHBr_3 is expressed as the product of its transfer coefficient (k_w) and the
213 concentration gradient (Δc) (Eq. (3)). The gradient is between the water concentration (c_w) and
214 theoretical equilibrium water concentration (c_{atm}/H), where c_{atm} is the atmospheric concentration
215 and H is Henry's law constant (Moore et al., 1995a; Moore et al., 1995b).

$$216 \quad F = k_w \cdot \Delta c = k_w \cdot \left(c_w - \frac{c_{\text{atm}}}{H} \right) \quad (3)$$

217 The compound-specific transfer coefficient (k_w) is determined using the air-sea gas exchange
218 parameterization of Nightingale et al. (2000) (Eq. (4))

$$219 \quad k_w = k \cdot \sqrt{Sc} / 660 \quad (4)$$

220 The transfer coefficient k is a function of the wind speed at 10 m height (u_{10}): $k = 0.2u_{10}^2 + 0.3u_{10}$,
221 and the Schmidt number (Sc) is a function of sea surface temperature (SST) from Quack and
222 Wallace (2003), which is expressed as $Sc = 4662.8 - 319.45 \cdot SST + 9.9012 \cdot SST^2 +$
223 $0.1159 \cdot SST^3$.

224 In this study, we use the CHBr_3 sea-to-air flux climatology from Ziska et al. (2013) as marine
225 background emissions. The global emission scenario from Ziska et al. (2013) is a bottom-up
226 estimate of the oceanic CHBr_3 fluxes, generated from atmospheric and oceanic surface ship-borne
227 *in situ* measurements between 1979 to 2013. Due to the paucity of data the 35 year mean gridded
228 data set was filled by inter- and extrapolating the *in situ* measurement data. The oceanic emissions
229 were calculated with the transfer coefficient parameterization of Nightingale et al. (2000) and 6-
230 hourly meteorological data, which allow a temporal emission variability related to wind and
231 temperature.

232

233 **2.4 FLEXPART**

234

235 To quantify the atmospheric impact of CHBr_3 emissions from macroalgae farming, the Lagrangian
236 particle dispersion model FLEXPART (Pisso et al., 2019) is used. FLEXPART has been evaluated
237 extensively in previous studies (e.g., Stohl et al., 1998; Stohl and Trickl, 1999). The model includes
238 moist convection and turbulence parameterizations in the atmospheric boundary layer and free
239 troposphere (Forster et al., 2007; Stohl and Thomson, 1999). The European Centre for Medium-
240 Range Weather Forecasts (ECMWF) reanalysis product ERA-Interim (Dee et al., 2011) with a



241 horizontal resolution of $1^\circ \times 1^\circ$ and 60 vertical model levels is used for the meteorological input
242 fields, providing air temperature, winds, boundary layer height, specific humidity, as well as
243 convective and large-scale precipitation with a 3-hour temporal resolution.

244 We conduct FLEXPART simulations for different emission scenarios as explained in the following
245 and summarized in Table 1:

246 1.) Australian scenarios: CHBr_3 emissions from the *Asparagopsis* farming in Geraldton, Triabunna,
247 and Yamba are calculated for an overall annual yield of 3.4674×10^4 Mg DW according to Equation
248 2. For the terrestrial systems, 5 day growth periods are assumed resulting in 73 harvests per year.
249 For the open ocean, the assumption of different growth periods results in three sub-scenarios a) 6
250 times 60 day growth periods with the first period starting on January 1st (referred to as GTY_O60),
251 b) one 96 day growth period starting on January 1st (GTY_O96_Jan), and c) and another starting
252 on July 1st (GTY_O96_Jul).

253 For the last Australian scenario, we assume that all farms are located around Darwin in the
254 Northern Territory tropics with 6 times 60 day growth periods in the open ocean and 73 times 5
255 day growth periods in the terrestrial systems (Darwin_O60). While this is an unlikely scenario
256 according to current plans, it is useful to demonstrate the influence of potential farming locations
257 on their environmental impact.

258 2.) Global scenarios: Emissions from *Asparagopsis* farming in Geraldton, Triabunna, and Yamba
259 are estimated according to the annual yield, upscaled by a factor of 30 to global requirements.
260 amounting to 1.04×10^6 Mg DW. Growth periods and harvesting frequencies are set up in the same
261 way as for the Australian scenarios. Short names of the global scenarios are the same as for the
262 Australian scenarios with the additional label 30x.

263 3) Background scenario: Emission from Ziska et al. (2013) for the entire coastal region around
264 Australia defined as all $1^\circ \times 1^\circ$ grid cells directly neighbouring the coastline (Ziska_Coast).

265 4.) Extreme event scenarios: We assume extreme conditions where a hypothetical tropical cyclone
266 causes implausible release of all CHBr_3 from the macroalgae farm and water into the atmosphere.
267 We focus on the case study of Geraldton and the tropical cyclone Joyce, which occurred from 6-
268 13 January 2018 around western Australia. We base the amount of available macroalgae biomass
269 on the Australian scenario and assume that the entire CHBr_3 content of all *Asparagopsis* at this
270 location is released at once. The two scenarios defined here assume that the tropical cyclone occurs
271 at the end of the 60 day growth period (Geraldton_Ex60) resulting in the release of 41.8 Mg CHBr_3



272 (21.7 mg $\text{CHBr}_3/\text{g DW}$ * 1926 Mg DW) or at the end of the 96 day growth period (Geraldton_Ex96)
273 resulting in the release of 250.8 Mg CHBr_3 (21.7 mg $\text{CHBr}_3/\text{g DW}$ * 1.1558×10^4 Mg DW).

274

275 The daily model output is recorded for all simulations. For the extreme event, which assumes the
276 destruction of a farm (Geraldton-Ex), the 3 hourly output is recorded. For all simulations, except
277 the background scenario and extreme scenario, trajectories are released from four regions of the
278 size of: a) Geraldton (open ocean, 11558 ha): $0.1^\circ \times 0.1^\circ$; b) Triabunna (open ocean, 4623 ha):
279 $0.06^\circ \times 0.06^\circ$; c) Triabunna (terrestrial systems, 126 ha): $0.01^\circ \times 0.01^\circ$; and d) Yamba (terrestrial
280 systems, 210 ha): $0.01^\circ \times 0.01^\circ$. For the tropical and extreme scenarios, trajectories are released
281 from the Darwin and Geraldton farms, respectively. For the background scenario Ziska_Coast,
282 trajectories are released from the $1.0^\circ \times 1.0^\circ$ grid along the Australian coastline. The amount of
283 released CHBr_3 is evenly distributed among the trajectories and is depleted during the Lagrangian
284 simulations according to the atmospheric half-life of 17 days (*e*-folding lifetime of 24 days)
285 (Hossaini et al., 2010; Montzka and Reimann, 2010).

286

287

288

289

290



291 **Table 1.** Detailed information on the scenarios set up for the atmospheric transport simulations
 292 with FLEXPART (Geraldton, Triubanna, and Yamba: GTY)

Name		Total Yield (Mg DW)	CHBr ₃ Emissions (Mg)	Notes	Simulation Period
Australian Scenarios	GTY_O60	Total: 34674	Total: 27.3	6 harvests (every 60 days) in the open ocean; 73 harvests (every 5 days) in the terrestrial systems.	01.01.2018 - 31.12.2018
	GTY_O96_Jan	Open Ocean: G: 11558 T: 4623 Y: -	Open Ocean: G: 9.10 T: 3.64	1 harvest (after 96 days) in open ocean; 73 harvests (every 5 days) in terrestrial systems. Growth in open ocean starts from 01.01.2018.	
	GTY_O96_Jul	Terrestrial systems: G: - T: 6935 Y: 11558	Terrestrial systems: T: 5.46 Y: 9.10	Same as GTY_O96_Jan but with growth in open ocean starting from 01.07.2018.	
	Darwin_O60	Total: 34674 Open Ocean: Darwin: 16181 Terrestrial systems: Darwin: 18493	Total: 27.3 Open Ocean: Darwin: 12.7 Terrestrial systems: Darwin: 14.6	Same as GTY_O60 but with farms near Darwin	
Global Scenarios	GTY_O60_30x	Total: 1.04022×10^6	Total: 819	Same as GTY_O60 but with initial biomass and areas 30 times larger.	2-month spin-up
	GTY_O96_Jan_30x	Open Ocean G: 3.4674×10^5 T: 1.3869×10^5 Y: -	Open Ocean G: 273 T: 109.2	Same as GTY_O96_Jan but with initial biomass and areas 30 times larger.	
	GTY_O96_Jul_30x	Terrestrial systems: G: - T: 2.0805×10^5 Y: 3.4674×10^5	Terrestrial systems: T: 163.8 Y: 273	Same as GTY_O96_Jul but with initial biomass and areas 30 times larger.	
	Darwin_O60_30x	Total: 1.04022×10^6 Open Ocean Darwin: 4.8543×10^5	Total: 819 Open Ocean Darwin: 381 Terrestrial systems: Darwin: 438	Same as Darwin_O60 but with initial biomass and areas 30 times larger.	



		Terrestrial systems: Darwin: 5.5479×10^5			
Background Scenario	Ziska_Coast	-	3109	CHBr ₃ emission of the coastal region of Australia from Ziska et al. (2013)	
Extreme Scenarios	Geraldton_Ex60	Open Ocean: G: 1926	Open Ocean: G: 41.8	Extreme event: CHBr ₃ in Geraldton surface water before harvest is released due to tropical cyclone Joyce (07.01.2018 – 15.01.2018). Harvest period: 60 days.	9.01.2018 – 9.02.2018 No spin-up
	Geraldton_Ex96	Open Ocean: G: 11558	Open Ocean: G: 250.8	Same as Geraldton_Ex60 but with harvest period of 96 days	

293

294

295

2.5 Ozone Depletion Potential (ODP)

296

297 The ozone depletion potential (ODP) is defined as the time-integrated potential destructive effect
 298 of a substance to the ozone layer relative to that of the reference substance CFC-11 (Wuebbles,
 299 1983). The ODP is a well-established and extensively used concept traditionally defined for
 300 anthropogenic long-lived halogens. However, the concept has been also applied to VSLSS
 301 (Brioude et al., 2010; Pisso et al., 2010): unlike the ODP for long-lived halocarbons, which is one
 302 constant number, the ODP of a VSLSS is a function of time and location of the emissions. This
 303 variable number still describes the time-integrated ozone depletion resulting from a CHBr₃ unit
 304 mass emission relative to the ozone depletion resulting from a unit mass emission of CFC-11.
 305 However, the trajectory-derived ODP of e.g. CHBr₃ is calculated as a function of location and time
 306 of the potential emissions. As for the classical ODP, and independently of the total amount of
 307 CHBr₃ emitted, the time and space dependent ODP describes only its potential but not the actual
 308 damaging effect to the ozone layer. The fraction of originally emitted VSLSSs reaching the
 309 stratosphere depends strongly on the meteorological conditions. In particular, it shows a
 310 pronounced seasonality. Here we apply ODP values adapted from Pisso et al. (2010), originally
 311 calculated for a VSLSS with a lifetime very similar to that of CHBr₃. ODPs for VSLSSs are calculated
 312 by means of combining two sources of information: one corresponding to the slow stratospheric
 313 branch and the other to the fast tropospheric branch of transport. The former is uniform for all
 314 species modelled and is based on the calculation of the expected stratospheric residence time of a
 315 Lagrangian particle entering the stratosphere. The latter is based on the probability of stratospheric



316 injection of a given unit emission of the tracer at the ground. The probability of injection depends
317 not only on the fraction of air reaching the tropopause but also on the time the air mass takes from
318 the ground to the tropopause. This is because during the transit of the air mass through the
319 troposphere, the precursor is chemically degraded, and the solubility of the products leads to mass
320 loss due to wet deposition.

321 In this study, we present the ODP-weighted emissions, which combine the information of the ODP
322 and surface emissions and are calculated by multiplying the CHBr_3 emissions with the trajectory-
323 derived ODP at each grid point. The ODP-weighted emissions provide insight in where and when
324 CHBr_3 is emitted that impacts stratospheric ozone (Tegtmeier et al., 2015). The absolute values
325 are subject to relatively large uncertainties arising from uncertainties in the parameterization of the
326 convective transport. Furthermore, the here applied ODP values do not consider product gas
327 entrainment and provide therefore a lower limit of the impact of CHBr_3 on stratospheric ozone.
328 Taking into account product gas entrainment can lead to 30% higher ODP values (Engel and Rigby,
329 2018; Tegtmeier et al., 2020), but has no large impact on the here presented comparison of global
330 ODP-weighted CHBr_3 emissions with farm-based ODP-weighted CHBr_3 emissions.

331

332 **3. CHBr_3 Emission and Atmospheric Mixing Ratio**

333

334 **3.1 CHBr_3 Emissions**

335

336 As shown in Eq. (2), the total CHBr_3 emissions are determined by the growth rate, growth period
337 and initial biomass. For our scenarios based on selected fixed growth rates, the growth periods are
338 adjusted so that the intended annual yield ($\sim 3.5 \times 10^4$ Mg DW) is achieved. We conduct a sensitivity
339 study to analyze how much the total emissions change for variations of the length and number of
340 the growth periods for a fixed annual yield. For this purpose, we compare Geraldton farming for
341 GTY_O60 (open ocean, six 60 day growth periods) with Geraldton farming for GTY_O96 (open
342 ocean, one 96 day growth period) and Yamba farming for GTY_O60 (terrestrial systems, 73
343 growth periods of 5 days). Our estimates reveal that the annual release of CHBr_3 from
344 *Asparagopsis* is the same for all three case studies (Fig. 3a), indicating that for a fixed annual yield
345 and growth rate, the culture conditions of open ocean and tank farming are not important for
346 VSLSS emissions.

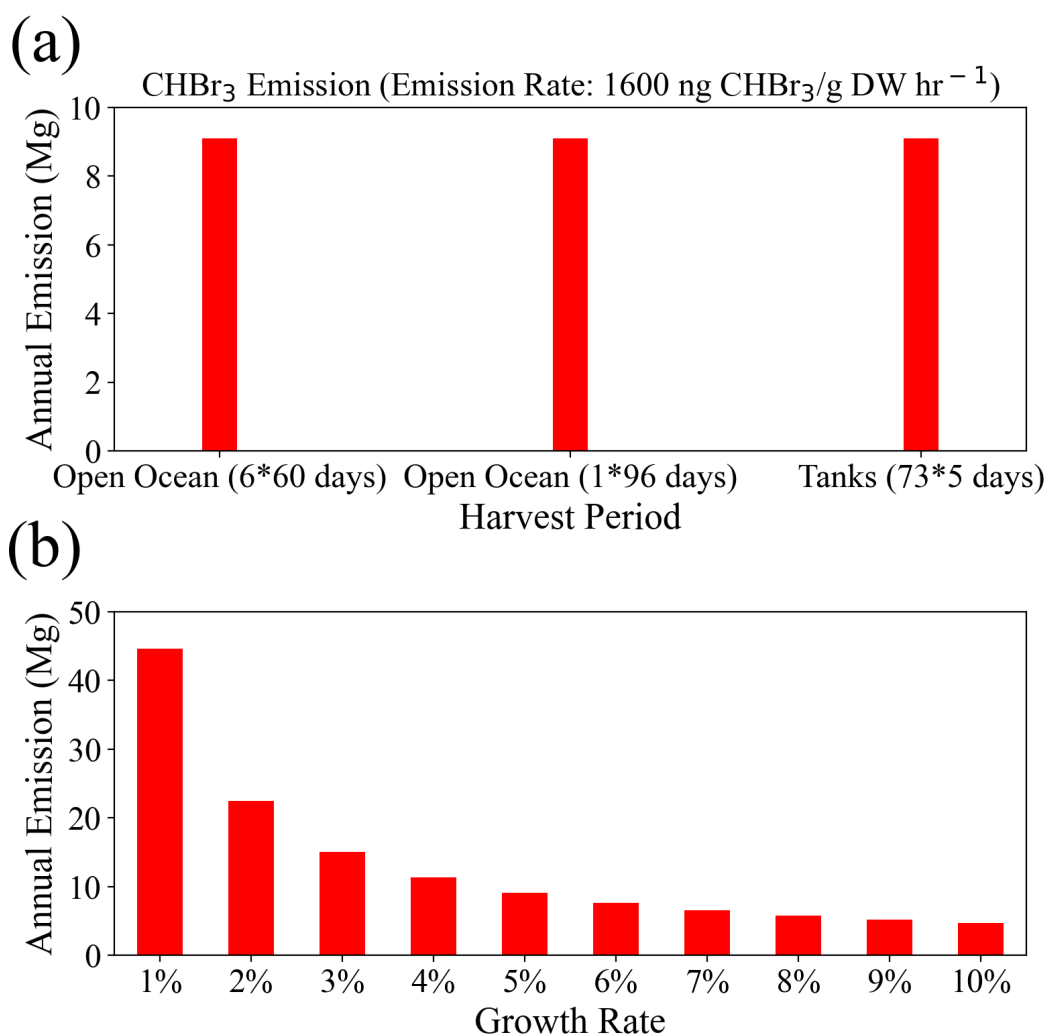


347 A second sensitivity study investigates the variations of CHBr_3 emissions for different growth rates
348 and the same fixed annual yield. For this purpose, we compare Geraldton farming (open ocean,
349 with an intended annual yield of $\sim 1.1 \times 10^4$ Mg DW) for different growth rates varying between 1%
350 and 10%. The scenario with a 5% growth rate corresponds to Geraldton farming for GTY_O60
351 (open ocean, six 60 day growth periods), while for the other growth rates the growth periods have
352 been adjusted to achieve the same annual yield.

353 The CHBr_3 emissions depend strongly on the growth rates (Fig 3b), with emission calculated for
354 a 1% growth rate being almost 10 times higher than the emissions calculated for a 10% growth
355 rate. For a lower growth rate, the initial biomass needs to be higher to achieve the targeted seaweed
356 yield ($\sim 1.1 \times 10^4$ Mg) after one year and/or the growth period needs to be longer, thus resulting in
357 larger amounts of biomass in the ocean and higher annual CHBr_3 emissions. Vice versa, for higher
358 growth rates, the annual oceanic biomass is smaller and total emissions are lower.

359 The overall emissions from the intended Australian seaweed farming of $\sim 3.5 \times 10^4$ Mg DW range
360 from 13.5 Mg (0.05 Mmol) for a 10% growth rate to 134 Mg (0.5 Mmol) per year for a 1% growth
361 rate. For the growth rates higher than 5%, the differences of CHBr_3 emissions are less significant
362 than those derived for the lower growth rates. In our study, we choose 5% growth rate as
363 representative, which leads to emissions of ~ 27 Mg (0.1 Mmol) CHBr_3 per year for the targeted
364 final yield. For the global scenario with an annual yield of $\sim 1.0 \times 10^6$ Mg DW (30 times of the
365 Australian target), the emissions would range from 412 Mg (1.6 Mmol) to 4014 Mg (16 Mmol)
366 per year, with the annual emission of 810 Mg (3.2 Mmol) for 5% growth rates.

367 Interestingly, the potential local emissions for all the farming scenarios are generally 3 to 6 orders
368 of magnitude higher than the background coastal emissions. The maximum climatological
369 emissions derived from available observations (Ziska_Coast) are around $2000 \text{ pmol m}^{-2} \text{ hr}^{-1}$ for
370 the coastal waters of Australia, while the emissions from an *Asparagopsis* farm can reach more
371 than $2.0 \times 10^6 \text{ pmol (2 } \mu\text{mol) m}^{-2} \text{ hr}^{-1}$ from a terrestrial system and more than $5.0 \times 10^5 \text{ pmol m}^{-2} \text{ hr}^{-1}$
372 ¹ from the open ocean. These differences are to a large degree related to the fact that the
373 Ziska_Coast is given on a $1.0^\circ \times 1.0^\circ$ grid, with high coastal values averaging out over the relatively
374 wide grid cells, while the values derived for the farms apply to much smaller areas. Tank emission
375 rates ($0.01^\circ \times 0.01^\circ$) and open ocean farming emission rates ($0.1^\circ \times 0.1^\circ$) averaged over a $1^\circ \times 1^\circ$ grid
376 cell result in $200 \text{ pmol CHBr}_3 \text{ m}^{-2} \text{ hr}^{-1}$ and $5000 \text{ pmol CHBr}_3 \text{ m}^{-2} \text{ hr}^{-1}$, respectively, thus being very
377 similar to the Ziska emissions.



378
379

380 **Figure 3.** The annual release of CHBr₃ (Mg yr⁻¹) from: a) same growth rate (5%) for different
381 growth periods; and b) under different growth rates, both with a total annual yield of 1.1558×10⁴
382 Mg DW.

383
384
385
386
387
388
389
390



391
392
393

3.2 Atmospheric CHBr_3 mixing ratio

394 We use the CHBr_3 emissions calculated in section 3.1 to simulate the atmospheric CHBr_3 mixing
395 ratios for each *Asparagopsis* farming scenario. Background CHBr_3 levels are calculated based on
396 the Ziska et al. (2013) Australian coastal emissions (Ziska_Coast). The temporal evolution of
397 CHBr_3 mixing ratio with height shows that the CHBr_3 resulting from the Australian farming
398 scenarios are negligible (see Figure S1) compared to the coastal background emissions of Australia
399 (Ziska_Coast).

400 However, for the global scenarios (Figure 4), atmospheric CHBr_3 is comparable to CHBr_3 resulting
401 from Australian coastal background emissions, especially near the end of the growth period in the
402 open ocean. For almost all scenarios (except for GTY_O96_Jul_30x), the emissions generally
403 reach higher into the atmosphere in the first three months of the year with enhanced values around
404 15 km, reflecting the stronger convection during austral summer. For open ocean emissions
405 occurring during late austral winter (GTY_O96_Jul_30x, Figure 4c), high CHBr_3 mixing ratios
406 are found around September, however at a lower altitude range compared to the equivalent
407 scenario with open ocean emission occurring during late austral summer (GTY_O96_Jan_30x;
408 Figure 3b).

409 The spatial distribution of annual mean CHBr_3 at 1 km (Figure 5) further confirms the
410 insignificance of the signals from the Australian farming scenarios compared with the background
411 CHBr_3 values. For the global scenarios, localized regions of high mixing ratios are found near the
412 locations of the farms due to the stronger emission. For Darwin_O60_30x, the belt of high mixing
413 ratios is extending northwestward, due to the prevailing easterlies in the tropics. At higher altitudes
414 (e.g., 5 km and 15 km; Figure S2-S3), localized high CHBr_3 is only found near Darwin for the
415 Darwin_O60_30x scenario, reflecting that strong tropical convection is needed to transport short
416 lived gases to such altitudes.

417 The results above suggest that in the boundary layer, global scenarios and extreme events could
418 lead to CHBr_3 comparable mixing ratios as those from the background scenario. Only in the global
419 tropical scenario (Darwin_O60_30x), CHBr_3 mixing ratios, which are larger than the background
420 values, can be found at high altitudes (Figure 4).

421 Simulations of the two extreme scenarios (Geraldton_Ex) for 60 and 96 day growth periods are
422 shown in Figure 6. For the Geraldton_Ex simulations, we assume the implausible scenario that

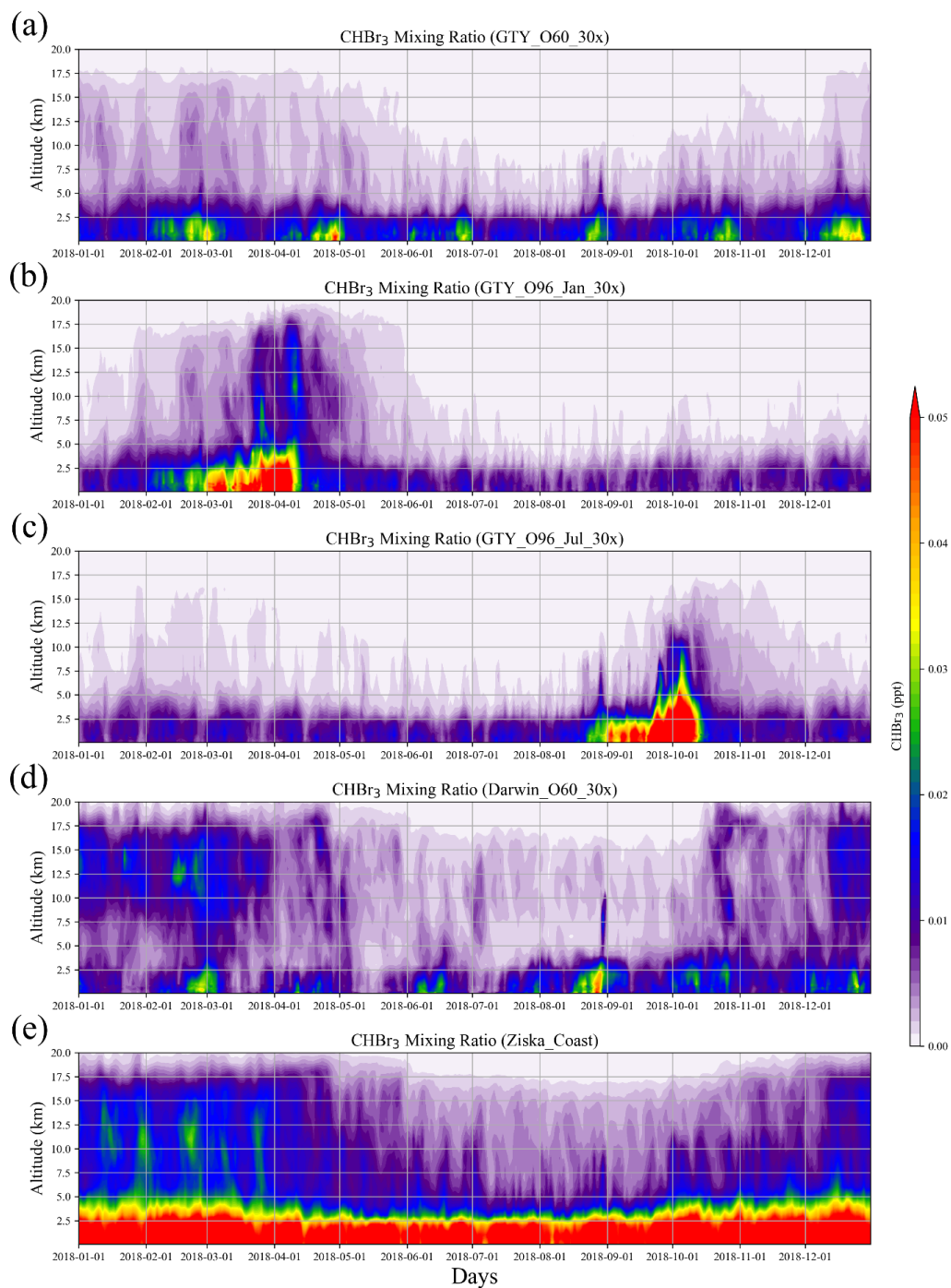


423 cyclone Joyce could destroy the farm on the day of harvest in January and the total CHBr_3 content
424 of the *Asparagopsis* stock was simultaneously released to the atmosphere during the event. Both
425 scenarios lead to significant CHBr_3 mixing ratios in the atmosphere, especially at altitudes below
426 5 km. Among the two scenarios, the Geraldton_Ex96 contributes the larger amount of CHBr_3
427 emission, as the macroalgae experienced a longer growth period, so the biomass was higher and
428 had accumulated more CHBr_3 . When averaged over the same period (Jan 9-Jan 26, 2018), the
429 CHBr_3 mixing ratios from Geraldton_Ex96 are much larger than those from Ziska_Coast (Figure
430 6) below 5 km, and signals with comparable magnitudes are found at 15 km.

431 As mentioned in section 3.1, the local CHBr_3 emissions due to the seaweed cultivation are
432 generally higher than coastal emission given on 1.0×1.0 grid. However, due to the relatively small
433 spatial extent of the farms, the emissions quickly dilute in the atmosphere, and the magnitude of
434 the mixing ratios decline rapidly off the coast and vertically.

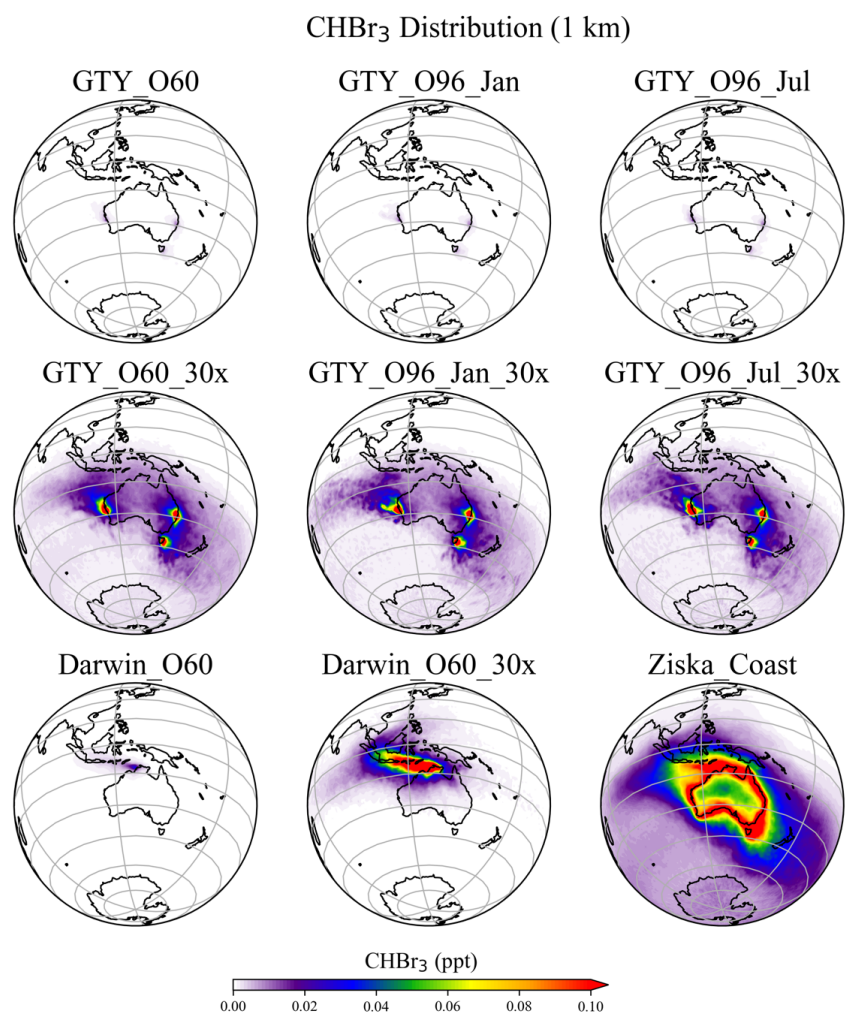
435

436

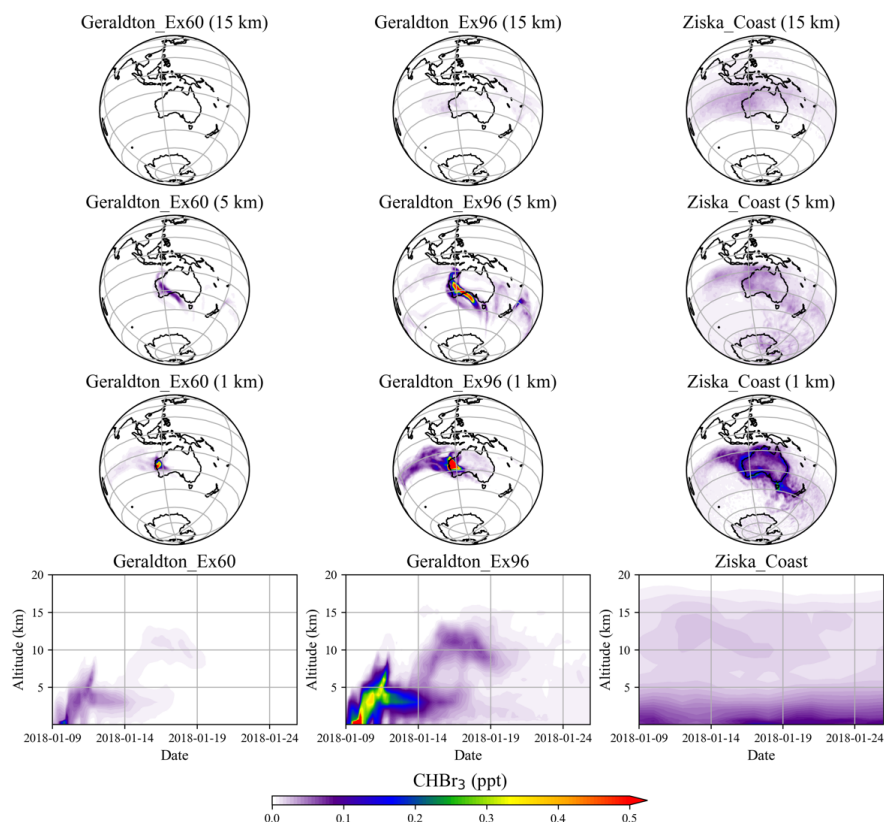




438 **Figure 4.** Altitude-time cross-sections of CHBr_3 averaged over $[10^\circ\text{-}45^\circ \text{ S}, 105^\circ\text{-}165^\circ \text{ E}]$ of
439 CHBr_3 mixing ratio from a) GTY_O60_30x, b) GTY_O96_Jan_30x, c) GTY_O96_Jul_30x, d)
440 Darwin_O60_30x, and e) Ziska_Coast.
441



442 **Figure 5.** Annual mean CHBr_3 spatial distribution from GTY_O60, GTY_O60_30x,
443 GTY_O96_Jan, GTY_O96_Jan_30x, GTY_O96_Jul, GTY_O96_Jul_30x, Darwin_O60,
444 Darwin_O60_30x, and Ziska_Coast at 1 km altitude.
445



446
447 **Figure 6.** 17-day average of spatial distribution and altitude-time cross-sections of CHBr₃ mixing
448 ratio averaged over [10°-45° S, 105°-165° E] for Geraldton_Ex60, Geraldton_Ex96, and
449 Ziska_Coast.

450
451
452 **4. Ozone depletion potential for CHBr₃**

453
454 The ODP distribution for the region around Australia, South-East Asia, and the Indian Ocean for
455 the Southern Hemisphere (SH) summer and winter is shown in Figure 7. The ODP distribution
456 changes strongly with season as the transport of short-lived halogenated substances such as CHBr₃
457 depends on the seasonal variations of the location of the Intertropical Convergence Zone (ITCZ).
458 Highest ODP values of 0.5, which imply that any amount (per mass) of CHBr₃ released from the
459 specific location will destroy half as much stratospheric ozone as the same amount of CFC-11
460 released from this location, are found during July over the Maritime continent and during January
461 over the West Pacific south of the equator. The northern Australian coastline shows highest ODP



462 values during January when the thermal equator and the ITCZ are shifted southwards and ODP
463 values for Yamba and Darwin are 0.26 and 0.29, respectively. The other two locations as well as
464 all four locations during SH winter, show ODP values of only up to 0.1.

465 As demonstrated in section 3, the total annual CHBr_3 emissions from any location are independent
466 of the details of the farming practice, however, the ODP-weighted emissions change for the
467 different scenarios as the growth periods fall into different seasons with varying ODP values. In
468 general, the scenario of one harvest period in SH summer leads to larger ODP-weighted emissions
469 when compared to the same biomass harvested throughout the year. In addition to the harvesting
470 practice, the locations of the farms have a large impact on the efficiency of the CHBr_3 transport to
471 the stratosphere and thus on the ODP-weighted emissions.

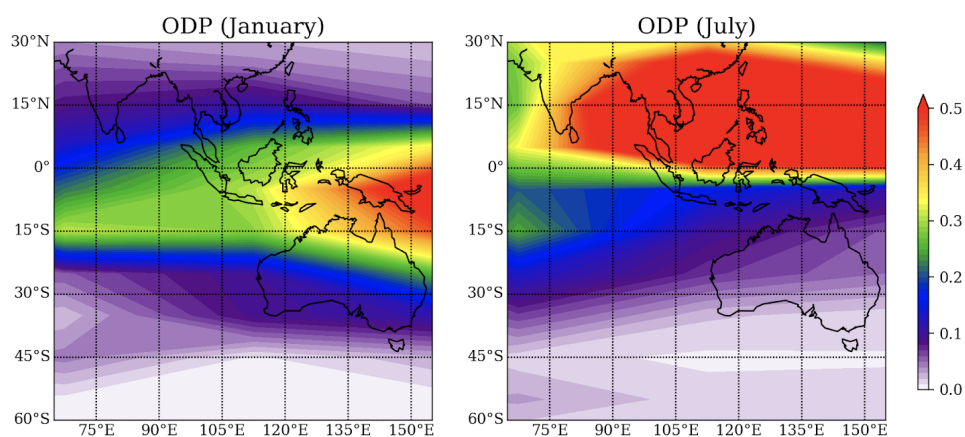
472 The ODP-weighted emissions of CHBr_3 for different emission scenarios are shown in Figure 8.
473 *Asparagopsis* farming at GTY (GTY_O60) leads to additional CHBr_3 emissions of up to 2.53 Mg
474 per year. If all farming ($\sim 3.5 \times 10^4$ Mg DW *Asparagopsis*) occurs in Darwin (Darwin_O60), ODP-
475 weighted emissions would increase to 6.48 Mg CHBr_3 per year. In comparison, all naturally
476 occurring emissions around the Australian coastline (Ziska_coast) lead to ODP-weighted CHBr_3
477 emissions of 221.52 Mg per year. In consequence, *Asparagopsis* farming in the three locations
478 Geraldton, Triabunna and Yamba would lead to an increase of the ODP-weighted emissions from
479 Australian coastal emissions of 1.14%. If all farming would take place in Darwin, ODP-weighted
480 CHBr_3 emissions would increase by 2.93%.

481 As the global ODP-weighted emissions were estimated to be around 4.0×10^4 Mg per year
482 (Tegtmeier et al., 2015), the additional contribution due to the Australian farming scenarios in
483 GTY or Darwin would be negligible increasing the contribution of CHBr_3 emissions to ozone
484 depletion by 0.006% and 0.016%, respectively. Even if the farming would be upscaled to cover
485 the global needs ($\sim 1.0 \times 10^6$ Mg DW), the ODP-weighted CHBr_3 emissions would only increase to
486 75 Mg and 195 Mg for farming in GTY (GTY_O60_30x) and Darwin (Darwin_O60_30x),
487 respectively. Thus produced CHBr_3 would increase the current contribution of CHBr_3 to
488 stratospheric ozone depletion by 0.19% and 0.48%, which is again a very small contribution.

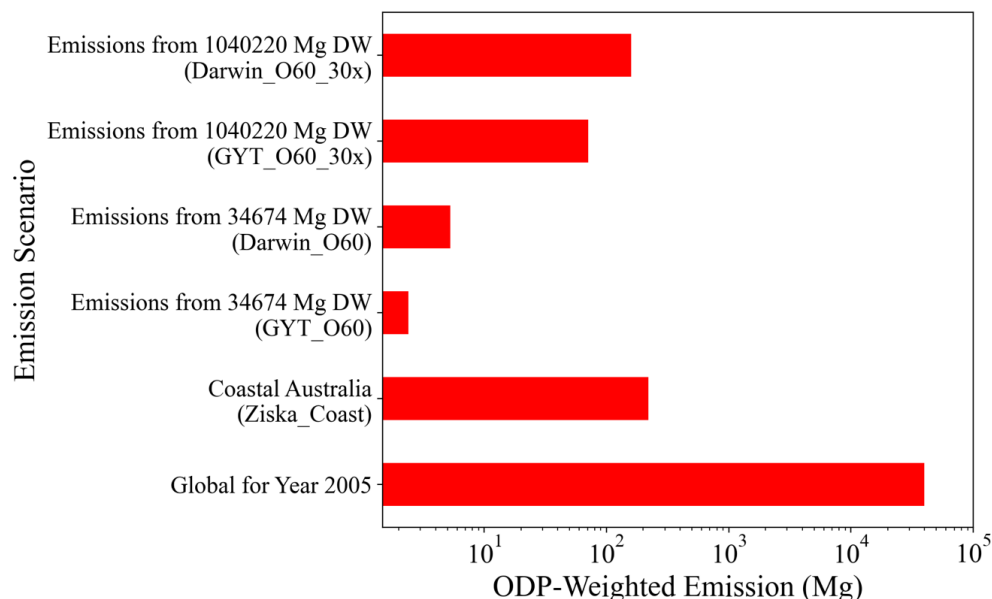
489 To assess the increase of the ODP-weighted CHBr_3 emissions under the most extreme and
490 implausible conditions, we envision the total harvest of one year, which contains 752 Mg (21.7
491 mg $\text{CHBr}_3/\text{g DW} * 3.4674 \times 10^4$ Mg DW) CHBr_3 , stored in a warehouse of 50 x 25 x 5 m in either
492 of the four locations. We assume that the facility is destroyed, and all 750 Mg released to the



493 atmosphere. Then maximum ODP-weighted CHBr_3 emissions would occur for the release in
494 Darwin during January and amount to 215.9 Mg almost doubling the ODP-weighted coastal CHBr_3
495 emissions of Australia. If the entire content of $\sim 1.0 \times 10^6$ Mg *Asparagopsis* DW (21.7 mg CHBr_3 /g
496 DW $\times 1.04022 \times 10^6$ Mg DW = 2.2573×10^4 Mg CHBr_3) would be released in Darwin, the additional
497 contribution of CHBr_3 to global ozone depletion could reach 16%.
498



499
500 **Figure 7.** Spatial distribution of the ODP in January and July.
501



502
503

504 **Figure 8.** The ODP-weighted emissions of CHBr_3 for different emission scenarios of
505 *Asparagopsis* farming, incidental content release scenarios and from global and coastal Australian
506 emissions, note that the x-axis is exponential.

507
508

509 5. Summary and Conclusions

510

511 In this study, we assessed the potential risks of CHBr_3 released from *Asparagopsis* farming near
512 Australia for the stratospheric ozone layer by analyzing different cultivation scenarios. We
513 conclude that the intended operation of *Asparagopsis* seaweed cultivation farms with an annual
514 yield of 3.4674×10^4 Mg DW in either open ocean or terrestrial cultures at the locations Triubanna,
515 Yamba, Geraldton, and Darwin will not impact the ozone layer under normal operating conditions.
516 For Australia scenarios with an annual yield of $\sim 3.5 \times 10^4$ Mg DW and algae growth rate of 5% per
517 day, the expected annual CHBr_3 emission from the considered *Asparagopsis* farms into the
518 atmosphere (~ 27 Mg, 0.11 Mmol) is less than 0.9% of the coastal Australian emissions (~ 3109
519 Mg, 12.3 Mmol). This contribution is negligible from a global perspective by adding less than
520 0.01% to the worldwide CHBr_3 emissions from natural and anthropogenic sources. The overall
521 emissions from the farms would be even smaller with a faster growth rate for the same annual
522 yield. We have assumed a high CHBr_3 production of 21.7 mg/g DW from superior strains and



523 expected lower CHBr_3 production of 14 mg/g DW would likewise reduce emissions to the
524 atmosphere.

525 The local CHBr_3 emissions from the *Asparagopsis* farms could be larger than emissions from
526 coastal Australia. However, the overall atmospheric impact of the *Asparagopsis* farms is negligible,
527 as the CHBr_3 dilutes rapidly and degrades in the atmosphere under normal weather conditions.
528 Mixing ratios of CHBr_3 are generally dominated by the coastal Australian emissions. In global
529 scenarios with annual yield $\sim 1.0 \times 10^6$ Mg DW, localized CHBr_3 mixing ratios comparable to the
530 background values can be found in the lower troposphere. In the upper troposphere, on the other
531 hand, mixing ratios larger than background values only appear in the global tropical scenario
532 (Darwin_O60_30x). The release of the complete CHBr_3 content from the macroalgae to the
533 environment on very short timescales (e.g., days) due to extreme weather situations could
534 contribute significant amounts to the atmosphere, especially during times when the standing stock
535 biomass is relatively large (Geraldton_Ex96). While such extreme scenarios could lead to much
536 larger mixing ratios than background values, such mass release events are implausible because
537 even if a farm was totally destroyed the seaweed stock could not instantaneously release all the
538 accumulated CHBr_3 . Such scenarios have been included here to evaluate a catastrophic and likely
539 impossible worst-case scenario.

540 The impact of CHBr_3 from the proposed seaweed farms on the stratospheric ozone layer is assessed
541 by weighting the emissions with the ozone depletion potential of CHBr_3 . In total, Australia
542 scenarios could lead to additional ODP-weighted CHBr_3 emissions of up to 2.53 Mg per year with
543 farms located in Geraldton, Triubana and Yamba. With all farming performed in Darwin
544 (Darwin_O60), the emitted CHBr_3 could reach the stratosphere on shorter time scales and ODP-
545 weighted emissions would increase to 6.48 Mg, which is less than 0.016% of the global ODP-
546 weighted emissions. For global tropical scenario (Darwin_O60_30x), the ODP-weighted
547 emissions amount to 175 Mg, increasing the global ozone depletion by 0.48%, resulting in a very
548 small contribution.

549 We note that all data characterizing the potential systems for the production of *Asparagopsis* are
550 based on few available literature data, lab scale tests and relatively small-scale field trials. This not
551 only places limitations on the technological representativeness of a future system and the temporal
552 validity of the study, but also demonstrates importance for directed studies, especially on the
553 release of CHBr_3 from *Asparagopsis* during cultivation. As this understanding evolves so will the



554 cultivation and processing technologies engineered to conserve the antimethanogenic CHBr_3 in
555 the seaweed biomass which is the primary value feature of *Asparagopsis*. These limitations are
556 largely mitigated in our study by evaluating various environmental and meteorological conditions
557 ranging from conservative to most extreme scenarios and by investigating different farming
558 practices based on various sensitivity studies.

559

560 **Data availability**

561 The CHBr_3 emission data and FLEXPART output can be obtained from the authors on request via
562 BQ (bquack@geomar.de), ST (susann.tegtmeier@usask.ca), or YJ (yue.jia@noaa.gov).

563

564 **Author Contributions**

565 BQ initialized the idea. YJ, BQ, and ST carried out the calculations and analysis. YJ performed
566 the FLEXPART simulations and produced the figures. YJ, BQ, and ST wrote the manuscript with
567 the contribution from other co-authors RK and IP. RK contributed to conceptualization, design,
568 writing, editing, procurement of funding. All the authors contributed to discussions and revisions
569 of the manuscript.

570

571 **Competing interests**

572 The authors declare that they have no conflict of interest.

573

574 **Acknowledgements**

575 The authors wish to acknowledge CSIRO, FutureFeed, and Sea Forest for their provision of
576 technical knowledge, data, and insight into *Asparagopsis* supply chains in Australia. The authors
577 would like to thank the European Centre for Medium-Range Weather Forecasts (ECMWF) for the
578 ERA-Interim reanalysis data and the FLEXPART development team for the Lagrangian particle
579 dispersion model used in this publication. The FLEXPART simulations were performed on
580 resources provided by the University of Saskatchewan.

581

582

583

584

585

586



587
588
589
590
591
592
593
594
595

Reference

596

597

598

599

600

601

602

603

604

605

606

607

608

609

610

611

612

613

614

615

616

617

618

619

620

621

622

623

624

625

626

627

628

629

630

631

632

Abbott, D. W., Aasen, I. M., Beauchemin, K. A., Grondahl, F., Gruninger, R., Hayes, M., Huws, S., Kenny, D. A., Krizsan, S. J., Kirwan, S. F., Lind, V., Meyer, U., Ramin, M., Theodoridou, K., von Soosten, D., Walsh, P. J., Waters, S., and Xing, X.: Seaweed and Seaweed Bioactives for Mitigation of Enteric Methane: Challenges and Opportunities, *Animals*, 10, 2432, <https://doi.org/10.3390/ani10122432>, 2020.

Aschmann, J., Sinnhuber, B. M., Atlas, E. L., and Schauffler, S. M.: Modeling the transport of very short-lived substances into the tropical upper troposphere and lower stratosphere, *Atmos. Chem. Phys.*, 9, 9237-9247, 10.5194/acp-9-9237-2009, 2009.

Battaglia, M. CSIRO and FutureFeed Pty Ltd. Personal Communication. 2020. <https://www.csiro.au/> and <https://www.future-feed.com/>

Beauchemin, K. A., Ungerfeld, E. M., Eckard, R. J., and Wang, M.: Review: Fifty years of research on rumen methanogenesis: lessons learned and future challenges for mitigation, *Animal*, 14, S2-S16, <https://doi.org/10.1017/S1751731119003100>, 2020.

Brioude, J., Portmann, R. W., Daniel, J. S., Cooper, O. R., Frost, G. J., Rosenlof, K. H., Granier, C., Ravishankara, A. R., Montzka, S. A., and Stohl, A.: Variations in ozone depletion potentials of very short-lived substances with season and emission region, *Geophysical Research Letters*, 37, <https://doi.org/10.1029/2010GL044856>, 2010.

Burreson, B. J., Moore, R. E., and Roller, P. P.: Volatile halogen compounds in the alga *Asparagopsis taxiformis* (Rhodophyta), *Journal of Agricultural and Food Chemistry*, 24, 856-861, 10.1021/jf60206a040, 1976.

Carpenter, L. J., and Liss, P. S.: On temperate sources of bromoform and other reactive organic bromine gases, *Journal of Geophysical Research: Atmospheres*, 105, 20539-20547, <https://doi.org/10.1029/2000JD900242>, 2000.

Carpenter, L. J., Reimann, S. (Lead Authors), Burkholder, J. B., Clerbaux, C., Hall, B. D., and Hossaini, R.: Ozone-depleting substances (ODSs) and other gases of interest to the Montreal Protocol. In: *Scientific assessment of ozone depletion: 2014. Global Ozone Research and Monitoring Project-Report A., E. and A., M. S. (Eds.)*, World Meteorological Organization., Geneva, Switzerland, 2014.



- 633
634 Dee, D. P., Uppala, S. M., Simmons, A. J., Berrisford, P., Poli, P., Kobayashi, S., Andrae, U.,
635 Balmaseda, M. A., Balsamo, G., Bauer, P., Bechtold, P., Beljaars, A. C. M., van de Berg, L., Bidlot,
636 J., Bormann, N., Delsol, C., Dragani, R., Fuentes, M., Geer, A. J., Haimberger, L., Healy, S. B.,
637 Hersbach, H., Holm, E. V., Isaksen, L., Kallberg, P., Kohler, M., Matricardi, M., McNally, A. P.,
638 Monge-Sanz, B. M., Morcrette, J. J., Park, B. K., Peubey, C., de Rosnay, P., Tavolato, C., Thepaut,
639 J. N., and Vitart, F.: The ERA-Interim reanalysis: configuration and performance of the data
640 assimilation system, *Q J Roy Meteor Soc*, 137, 553-597, <https://doi.org/10.1002/qj.828>, 2011.
- 641
642 Elsom, S. Sea Forest Asparagopsis production. Personal Communication.
643 <https://www.seaforest.com.au/>, 2020.
- 644
645 Engel, A., and M. Rigby (Lead Authors), J.B. Burkholder, R.P. Fernandez, L. Froidevaux, B.D.
646 Hall, R. Hossaini, T. Saito, M.K. Vollmer, and B. Yao, Update on Ozone-Depleting Substances
647 (ODSs) and Other Gases of Interest to the Montreal Protocol, Chapter 1 in Scientific Assessment
648 of Ozone Depletion: 2018, Global Ozone Research and Monitoring Project — Report No.
649 58, World Meteorological Organization, Geneva, Switzerland, 2018.
- 650
651 Forster, C., Stohl, A., and Seibert, P.: Parameterization of Convective Transport in a Lagrangian
652 Particle Dispersion Model and Its Evaluation, *Journal of Applied Meteorology and Climatology*,
653 46, 403-422, 10.1175/jam2470.1, 2007.
- 654
655 Gerber, P.J., Steinfeld, H., Henderson, B., Mottet, A., Opio, C., Dijkman, J., Falcucci, A. &
656 Tempio, G.: Tackling climate change through livestock – A global assessment of emissions and
657 mitigation opportunities. Food and Agriculture Organization of the United Nations (FAO), Rome,
658 2013.
- 659
660 Hense, I., and Quack, B.: Modelling the vertical distribution of bromoform in the upper water
661 column of the tropical Atlantic Ocean, *Biogeosciences*, 6, 535-544, 10.5194/bg-6-535-2009, 2009.
- 662
663 Herrero, M., Henderson, B., Havlik, P., Thornton, P. K., Conant, R. T., Smith, P., Wirsenius, S.,
664 Hristov, A. N., Gerber, P., Gill, M., Butterbach-Bahl, K., Valin, H., Garnett, T., and Stehfest, E.:
665 Greenhouse gas mitigation potentials in the livestock sector, *Nat Clim Change*, 6, 452-461,
666 10.1038/nclimate2925, 2016.
- 667
668 Herrero, M., and Thornton, P. K.: Livestock and global change: Emerging issues for sustainable
669 food systems, *Proceedings of the National Academy of Sciences*, 110, 20878-20881,
670 10.1073/pnas.1321844111, 2013.
- 671
672 Hossaini, R., Chipperfield, M. P., Monge-Sanz, B. M., Richards, N. A. D., Atlas, E., and Blake,
673 D. R.: Bromoform and dibromomethane in the tropics: a 3-D model study of chemistry and
674 transport, *Atmos. Chem. Phys.*, 10, 719-735, 10.5194/acp-10-719-2010, 2010.
- 675
676 Hung, L. D., Hori, K., Nang, H. Q., Kha, T., and Hoa, L. T.: Seasonal changes in growth rate,
677 carrageenan yield and lectin content in the red alga *Kappaphycus alvarezii* cultivated in Camranh
678 Bay, Vietnam, *Journal of Applied Phycology*, 21, 265-272, 10.1007/s10811-008-9360-2, 2009.



- 679
680 IPCC: Climate Change 2014: Synthesis Report. Contribution of Working Groups I, II and III to
681 the Fifth Assessment Report of the Intergovernmental Panel on Climate Change IPCC, Geneva,
682 Switzerland, 2014.
683
684 Kamra, D. N.: Rumen microbial ecosystem, *Curr Sci India*, 89, 124-135,
685 <http://www.jstor.org/stable/24110438>, 2005.
686
687 Kinley, R. D. and Fredeen, A. H.: In Vitro Evaluation of Feeding North Atlantic Stormtoss
688 Seaweeds on Ruminant Digestion. *Journal of Applied Phycology*, 27, 2387-2393.
689 <http://dx.doi.org/10.1007/s10811-014-0487-z>, 2015.
690
691 Kinley, R., Vucko, M., Machado, L., and Tomkins, N.: In Vitro Evaluation of the
692 Antimethanogenic Potency and Effects on Fermentation of Individual and Combinations of Marine
693 Macroalgae. *American Journal of Plant Sciences*, 7, 2038-2054. doi: 10.4236/ajps.2016.714184,
694 2016a.
695
696 Kinley, R. D., de Nys, R., Vucko, M. J., Machado, L., and Tomkins, N. W.: The red
697 macroalgae *Asparagopsis taxiformis* is a potent natural antimethanogenic that reduces methane
698 production during *in vitro* fermentation with rumen fluid, *Animal Production Science*, 56, 282-289,
699 <https://doi.org/10.1071/AN15576>, 2016b.
700
701 Kinley, R. D., Martinez-Fernandez, G., Matthews, M. K., de Nys, R., Magnusson, M., and
702 Tomkins, N. W.: Mitigating the carbon footprint and improving productivity of ruminant livestock
703 agriculture using a red seaweed, *Journal of Cleaner Production*, 259, 120836,
704 <https://doi.org/10.1016/j.jclepro.2020.120836>, 2020.
705
706 Leedham, E. C., Hughes, C., Keng, F. S. L., Phang, S. M., Malin, G., and Sturges, W. T.: Emission
707 of atmospherically significant halocarbons by naturally occurring and farmed tropical macroalgae,
708 *Biogeosciences*, 10, 3615-3633, 10.5194/bg-10-3615-2013, 2013.
709
710 Li, X. X., Norman, H. C., Kinley, R. D., Laurence, M., Wilmot, M., Bender, H., de Nys, R., and
711 Tomkins, N.: *Asparagopsis taxiformis* decreases enteric methane production from sheep, *Animal*
712 *Production Science*, 58, 681-688, <https://doi.org/10.1071/AN15883>, 2018.
713
714 Liang, Q., Stolarski, R. S., Kawa, S. R., Nielsen, J. E., Douglass, A. R., Rodriguez, J. M., Blake,
715 D. R., Atlas, E. L., and Ott, L. E.: Finding the missing stratospheric Br_y: a global
716 modeling study of CHBr₃ and CH₂Br₂, *Atmos. Chem.*
717 *Phys.*, 10, 2269-2286, 10.5194/acp-10-2269-2010, 2010.
718
719 Maas, J., Tegtmeier, S., Quack, B., Biastoch, A., Durgadoo, J. V., Ruhs, S., Gollasch, S., and
720 David, M.: Simulating the spread of disinfection by-products and anthropogenic bromoform
721 emissions from ballast water discharge in Southeast Asia, *Ocean Sci*, 15, 891-904, 10.5194/os-15-
722 891-2019, 2019.
723



- 724 Maas, J., Tegtmeier, S., Jia, Y., Quack, B., Durgadoo, J. V., and Biastoch, A.: Simulations of
725 anthropogenic bromoform indicate high emissions at the coast of East Asia, *Atmos. Chem. Phys.*,
726 21, 4103-4121, 10.5194/acp-21-4103-2021, 2021.
727
- 728 Machado, L., Magnusson, M., Paul, N. A., de Nys, R., and Tomkins, N.: Effects of Marine and
729 Freshwater Macroalgae on In Vitro Total Gas and Methane Production, *PLOS ONE*, 9, e85289,
730 10.1371/journal.pone.0085289, 2014.
731
- 732 Machado, L., Magnusson, M., Paul, N. A., Kinley, R., de Nys, R., and Tomkins, N. W.:
733 Identification of bioactives from the red seaweed *Asparagopsis taxiformis* that promote
734 antimethanogenic activity in vitro, *J. Appl. Phycol.*, 28, 3117-3126,
735 <https://doi.org/10.1007/s10811-016-0830-7>, 2016.
736
- 737 Magnusson, M., Vucko, M. J., Neoh, T. L., and de Nys, R.: Using oil immersion to deliver a
738 naturally-derived, stable bromoform product from the red seaweed *Asparagopsis taxiformis*, *Algal*
739 *Research*, 51, 102065, <https://doi.org/10.1016/j.algal.2020.102065>, 2020.
740
- 741 Mata, L., Gaspar, H., and Santos, R.: CARBON/NUTRIENT BALANCE IN RELATION TO
742 BIOMASS PRODUCTION AND HALOGENATED COMPOUND CONTENT IN THE RED
743 ALGA *ASPARAGOPSIS TAXIFORMIS* (BONNEMAISONIACEAE)1, *Journal of Phycology*,
744 48, 248-253, <https://doi.org/10.1111/j.1529-8817.2011.01083.x>, 2012.
745
- 746 Marshall, R. A., Harper, D. B., McRoberts, W. C., and Dring, M. J.: Volatile bromocarbons
747 produced by *Falkenbergia* stages of *Asparagopsis* spp. (Rhodophyta), *Limnology and*
748 *Oceanography*, 44, 1348-1352, doi: 10.4319/lo.1999.44.5.1348, 1999.
749
- 750 Mata, L., Lawton, R. J., Magnusson, M., Andreakis, N., de Nys, R., and Paul, N. A.: Within-
751 species and temperature-related variation in the growth and natural products of the red alga
752 *Asparagopsis taxiformis*, *Journal of Applied Phycology*, 29, 1437-1447, 10.1007/s10811-016-
753 1017-y, 2017.
754
- 755 Mayberry, D., Bartlett, H., Moss, J., Davison, T., and Herrero, M.: Pathways to carbon-neutrality
756 for the Australian red meat sector, *Agricultural Systems*, 175, 13-21,
757 <https://doi.org/10.1016/j.agsy.2019.05.009>, 2019.
758
- 759 Moate, P. J., Deighton, M. H., Williams, S. R. O., Pryce, J. E., Hayes, B. J., Jacobs, J. L., Eckard,
760 R. J., Hannah, M. C., and Wales, W. J.: Reducing the carbon footprint of Australian milk
761 production by mitigation of enteric methane emissions, *Animal Production Science*, 56, 1017-1034,
762 <https://doi.org/10.1071/AN15222>, 2016.
763
- 764 Moore, R. M., Geen, C. E., and Tait, V. K.: Determination of Henry's Law constants for a suite of
765 naturally occurring halogenated methanes in seawater, *Chemosphere*, 30, 1183-1191,
766 [https://doi.org/10.1016/0045-6535\(95\)00009-W](https://doi.org/10.1016/0045-6535(95)00009-W), 1995a.
767



- 768 Moore, R. M., Tokarczyk, R., Tait, V. K., Poulin, M., and Geen, C.: Marine phytoplankton as a
769 natural source of volatile organohalogenes. In: Naturally-Produced Organohalogenes, Grimvall, A.
770 and de Leer, E. W. B. (Eds.), Springer Netherlands, Dordrecht, 1995b.
771
- 772 Morgavi, D. P., Forano, E., Martin, C., and Newbold, C. J.: Microbial ecosystem and
773 methanogenesis in ruminants, *Animal*, 4, 1024-1036, 10.1017/s1751731110000546, 2010.
774
- 775 Montzka, S. A. and Reimann, S.: Ozone-depleting substances and related chemicals, in Scientific
776 Assessment of Ozone Depletion: 2010, Global Ozone Research and Monitoring Project – Report No.
777 52, WMO, Geneva, Switzerland, 2011.
778
- 779 Nightingale, P. D., Malin, G., and Liss, P. S.: Production of chloroform and other low molecular-
780 weight halocarbons by some species of macroalgae, *Limnology and Oceanography*, 40, 680-689,
781 <https://doi.org/10.4319/lo.1995.40.4.0680>, 1995.
782
- 783 Nightingale, P. D., Malin, G., Law, C. S., Watson, A. J., Liss, P. S., Liddicoat, M. I., Boutin, J.,
784 and Upstill-Goddard, R. C.: In situ evaluation of air-sea gas exchange parameterizations using
785 novel conservative and volatile tracers, *Global Biogeochemical Cycles*, 14, 373-387,
786 <https://doi.org/10.1029/1999GB900091>, 2000.
787
- 788 Patra, A. K.: Enteric methane mitigation technologies for ruminant livestock: a synthesis of current
789 research and future directions, *Environ Monit Assess*, 184, 1929-1952, 10.1007/s10661-011-2090-
790 y, 2012.
791
- 792 Paul, N. A., de Nys, R., and Steinberg, P. D.: Chemical defence against bacteria in the red alga
793 *Asparagopsis armata*: linking structure with function, *Marine Ecology Progress Series*, 306, 87-
794 101, 10.3354/meps306087, 2006.
795
- 796 Pisso, I., Haynes, P. H., and Law, K. S.: Emission location dependent ozone depletion potentials
797 for very short-lived halogenated species, *Atmos. Chem. Phys.*, 10, 12025-12036, 10.5194/acp-10-
798 12025-2010, 2010.
799
- 800 Pisso, I., Sollum, E., Grythe, H., Kristiansen, N. I., Cassiani, M., Eckhardt, S., Arnold, D., Morton,
801 D., Thompson, R. L., Groot Zwaafink, C. D., Evangeliou, N., Sodemann, H., Haimberger, L.,
802 Henne, S., Brunner, D., Burkhart, J. F., Fouilloux, A., Brioude, J., Philipp, A., Seibert, P., and
803 Stohl, A.: The Lagrangian particle dispersion model FLEXPART version 10.4, *Geosci. Model
804 Dev.*, 12, 4955-4997, 10.5194/gmd-12-4955-2019, 2019.
805
- 806 Quack, B., and Wallace, D. W. R.: Air-sea flux of bromoform: Controls, rates, and implications,
807 *Global Biogeochemical Cycles*, 17, <https://doi.org/10.1029/2002GB001890>, 2003.
808
- 809 Roque, B. M., Venegas, M., Kinley, R. D., de Nys, R., Duarte, T. L., Yang, X., and Kebreab, E.:
810 Red seaweed (*Asparagopsis taxiformis*) supplementation reduces enteric methane by over 80
811 percent in beef steers, *PLOS ONE*, 16, e0247820, 10.1371/journal.pone.0247820, 2021.
812



- 813 Sinnhuber, B.-M., and Meul, S.: Simulating the impact of emissions of brominated very short lived
814 substances on past stratospheric ozone trends, *Geophysical Research Letters*, 42, 2449-2456,
815 <https://doi.org/10.1002/2014GL062975>, 2015.
816
- 817 Stohl, A., Hittenberger, M., and Wotawa, G.: Validation of the lagrangian particle dispersion
818 model FLEXPART against large-scale tracer experiment data, *Atmospheric Environment*, 32,
819 4245-4264, [https://doi.org/10.1016/S1352-2310\(98\)00184-8](https://doi.org/10.1016/S1352-2310(98)00184-8), 1998.
820
- 821 Stohl, A. and Thomson, D.: A density correction for Lagrangian particle dispersion models,
822 *Boundary-Layer Meteorology*, 90, 155-167, [10.1023/A:1001741110696](https://doi.org/10.1023/A:1001741110696), 1999.
823
- 824 Stohl, A. and Trickl, T.: A textbook example of long-range transport: Simultaneous observation
825 of ozone maxima of stratospheric and North American origin in the free troposphere over Europe,
826 *Journal of Geophysical Research: Atmospheres*, 104, 30445-30462, [10.1029/1999JD900803](https://doi.org/10.1029/1999JD900803), 1999.
827
- 828 Tegtmeier, S., Ziska, F., Pisso, I., Quack, B., Velders, G. J. M., Yang, X., and Krüger, K.: Oceanic
829 bromoform emissions weighted by their ozone depletion potential, *Atmos. Chem. Phys.*, 15,
830 13647-13663, [10.5194/acp-15-13647-2015](https://doi.org/10.5194/acp-15-13647-2015), 2015.
831
- 832 Tegtmeier, S., Atlas, E., Quack, B., Ziska, F., and Krüger, K.: Variability and past long-term
833 changes of brominated very short-lived substances at the tropical tropopause, *Atmos. Chem. Phys.*,
834 20, 7103-7123, [10.5194/acp-20-7103-2020](https://doi.org/10.5194/acp-20-7103-2020), 2020.
835
- 836 Vucko, M. J., Magnusson, M., Kinley, R. D., Villart, C., and de Nys, R.: The effects of processing
837 on the in vitro antimethanogenic capacity and concentration of secondary metabolites of
838 *Asparagopsis taxiformis*, *J. Appl. Phycol.*, 29, 1577-1586, [10.1007/s10811-016-1004-3](https://doi.org/10.1007/s10811-016-1004-3), 2017.
839
- 840 Wuebbles, D. J.: Chlorocarbon Emission Scenarios - Potential Impact on Stratospheric Ozone,
841 *Journal of Geophysical Research-Oceans*, 88, 1433-1443, [10.1029/JC088iC02p01433](https://doi.org/10.1029/JC088iC02p01433), 1983.
842
- 843 Yang, X., Abraham, N. L., Archibald, A. T., Braesicke, P., Keeble, J., Telford, P. J., Warwick, N.
844 J., and Pyle, J. A.: How sensitive is the recovery of stratospheric ozone to changes in
845 concentrations of very short-lived bromocarbons?, *Atmospheric Chemistry and Physics*, 14,
846 10431-10438, [10.5194/acp-14-10431-2014](https://doi.org/10.5194/acp-14-10431-2014), 2014.
847
- 848 Yong, Y. S., Yong, W. T. L., and Anton, A.: Analysis of formulae for determination of seaweed
849 growth rate, *Journal of Applied Phycology*, 25, 1831-1834, [10.1007/s10811-013-0022-7](https://doi.org/10.1007/s10811-013-0022-7), 2013.
850
- 851 Ziska, F., Quack, B., Abrahamsson, K., Archer, S. D., Atlas, E., Bell, T., Butler, J. H., Carpenter,
852 L. J., Jones, C. E., Harris, N. R. P., Hepach, H., Heumann, K. G., Hughes, C., Kuss, J., Kruger, K.,
853 Liss, P., Moore, R. M., Orlikowska, A., Raimund, S., Reeves, C. E., Reifenhauer, W., Robinson,
854 A. D., Schall, C., Tanhua, T., Tegtmeier, S., Turner, S., Wang, L., Wallace, D., Williams, J.,
855 Yamamoto, H., Yvon-Lewis, S., and Yokouchi, Y.: Global sea-to-air flux climatology for
856 bromoform, dibromomethane and methyl iodide, *Atmospheric Chemistry and Physics*, 13, 8915-
857 8934, [10.5194/acp-13-8915-2013](https://doi.org/10.5194/acp-13-8915-2013), 2013.